ORGANIC LETTERS

2011
Vol. 13, No. 1
30−33

Switching Around Two Axles: Controlling the Configuration and Conformation of a Hydrazone-Based Switch

Xin Su and Ivan Aprahamian*

6128 Burke Laboratory, Department of Chemistry, Dartmouth College, Hanover, New Hampshire 03755, United States

ivan.aprahamian@dartmouth.edu

Received October 7, 2010

ABSTRACT

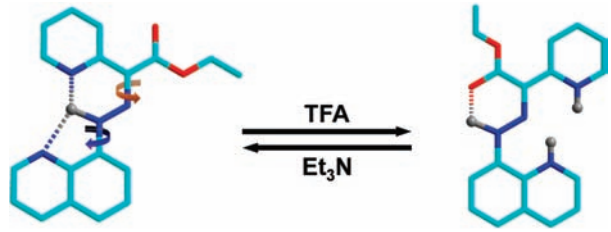

A hydrazone-based rotary switch, having a quinolinyl stator and a pyridine ring as part of the rotor, can be induced using pH to undergo a four-step switching sequence. This process yields three stable isomers and a fourth "metastable" one that can all be addressed separately based on the sequence of acid and base added. The switching process proceeds via conformational and/or configurational changes, allowing the molecule to rotate around two different axles.

Manipulating molecular motion[1] is at the heart of ongoing studies that aim at developing molecular machinery that will ultimately be used in advanced nanotechnology applications.[2] A diverse array of molecular systems that can be activated using various external stimuli, for example, chemical,[3] electrochemical,[4] and photochemical,[5] have been developed as part of this effort. The activated motion can be rotary in nature or linear depending on the targeted application. Synthetic rotary switches and motors are of particular interest as they resemble and mimic systems found in nature (e.g., ATPase synthase),[6] and these have been so far the only ones to produce unidirectional motion.[7] Chemically activated rotary switches depend on *conformational* changes in their function, whereas photochemically activated switches rely on *configurational* ones. There seems to be a significant break between these two approaches, and advancement of this field

(1) (a) Sauvage, J.-P., Ed. *Molecular Machines and Motors*, Springer, New York: 2001. (b) Feringa, B. L., Ed. *Molecular Switches*; Wiley-VCH: Weinheim, Germany, 2001. (c) Kay, E. R.; Leigh, D. A.; Zerbetto, F. *Angew. Chem., Int. Ed.* **2007**, *46*, 72–191. (d) Balzani, V.; Credi, A.; Venturi, M. *Molecular Decices and Machines - Concepts and Perspectives for the Nanoworld*; Wiley-VCH: Weinheim, Germany, 2008. (e) Michl, J.; Sykes, E. C. H. *ACS Nano* **2009**, *3*, 1042–1048. (f) Stoddart, J. F. *Chem. Soc. Rev.* **2009**, *38*, 1802–1820.

(2) (a) Collier, C. P.; Mattersteig, G.; Wong, E. W.; Luo, Y.; Beverly, K.; Sampaio, J.; Raymo, F. M.; Stoddart, J. F.; Heath, J. R. *Science* **2000**, *289*, 1172–1175. (b) Flood, A. H.; Stoddart, J. F.; Steuerman, D. W.; Heath, J. R. *Science* **2004**, *306*, 2055–2056. (c) Leigh, D. A.; Morales, M. A. F.; Pérez, E. M.; Wong, J. K. Y.; Saiz, C. G.; Slawin, A. M. Z.; Carmichael, A. J.; Haddleton, D. M.; Brouwer, A. M.; Buma, W. J.; Wurpel, G. W. H.; León, S.; Zerbetto, F. *Angew. Chem., Int. Ed.* **2005**, *44*, 3062–3067. (d) Hess, H. *Science* **2006**, *312*, 860–861. (e) Green, J. E.; Choi, J. W.; Boukai, A.; Bunimovich, Y.; Johnston-Halperin, E.; DeIonno, E.; Luo, Y.; Sheriff, B. A.; Xu, K.; Shin, Y. S.; Tseng, H.-R.; Stoddart, J. F.; Heath, J. R. *Nature* **2007**, *445*, 414–417. (f) Browne, W. R.; Feringa, B. L. *Annu. Rev. Phys. Chem.* **2009**, *60*, 407–428. (g) Omabegho, T.; Sha, R.; Seeman, N. C. *Science* **2009**, *324*, 67–71.

(3) (a) Badjić, J. D.; Balzani, V.; Credi, A.; Silvi, S.; Stoddart, J. F. *Science* **2004**, *303*, 1845–1849. (b) Berná, J.; Leigh, D. A.; Lubomska, M.; Mendoza, S. M.; Pérez, E. M.; Rudolf, P.; Teobaldi, G.; Zerbetto, F. *Nat. Mater.* **2005**, *4*, 704–710. (c) Bonnet, S.; Collin, J. P.; Koizumi, M.; Mobian, P.; Sauvage, J.-P. *Adv. Mater.* **2006**, *18*, 1239–1250. (d) Leblond, J.; Gao, H.; Petitjean, A.; Leroux, J.-C. *J. Am. Chem. Soc.* **2010**, *132*, 8544–8545.

10.1021/ol102422h
Published on Web 12/06/2010

will ultimately rely on our ability to control various types of motion in different parts of a single molecule.[8] Such a modulation of integrated molecular motion[9] will ultimately lead to complexity[10] and emergent phenomena.[11]

Previously we have reported how the configuration of a hydrazone-based switch[12] can be controlled by acid/base modulations. Inspired by this prototype, we designed a new switch **QPH-*E*** (Scheme 1) with the aim of chemically controlling both the configuration and conformation of a single molecule; a feat that to the best of our knowledge has not been accomplished so far. Here we describe the straightforward synthesis, characterization, and four-step switching of this novel tristable molecular switch. The protonation of **QPH-*E*** by trifluoroacetic acid (TFA) leads to **QPH-*Z*-**H^+, accompanied by a configurational change originating from the rotation about the C═N double bond. Further protonation leads to rotation about the C−N single bond, generating a new conformational isomer, **QPH-*Z*-**H_2^{2+}, that *retains* the *Z* configuration. After deprotonation with triethylamine (Et_3N), both **QPH-*Z*-**H^+ and **QPH-*Z*-**H_2^{2+} convert into a neutral metastable species **QPH-*Z***, which eventually equilibrates to give back the thermodynamically more stable **QPH-*E*** isomer. The configuration and conformation of the system can be modulated based on the sequence at which the acid and base are added, leading to a switch that can be prompted to rotate around two different axles.

Hydrazone **QPH** was synthesized by the coupling of the diazonium salt derived from 8-aminoquinoline with ethyl-2-pyridylacetate (see SI Scheme S1, Supporting Information). The crystal structure of **QPH-*E*** (see SI Figure X-ray S1, Supporting Information) shows a near planar geometry[13] as expected[14] and a strong H-bond between the N−H proton and the pyridyl nitrogen atom (N−H···N, 2.6162(20) Å, 130.537(101)°) and another weaker H-bond with the quinolinyl nitrogen atom (N−H···N, 2.7070(21) Å, 102.821(101)°). This molecular geometry of **QPH-*E*** is also consistent with the ^{1}H NMR spectrum, which shows a characteristic hydrazone N−H signal at 15.39 ppm (Figure 1a), indicating that this proton is H-bonded with the pyridyl nitrogen atom and that it is under the influence of the ring current effect of the quinolinyl group.[12] The fully ^{1}H NMR spectrum (see SI Figures S1−6, Supporting Information) also shows the presence of **QPH-*Z*** in solution; the *E*:*Z* isomer ratio is 82:18 in CD_3CN.[15]

Scheme 1. Schematic Illustration of the Switching Process

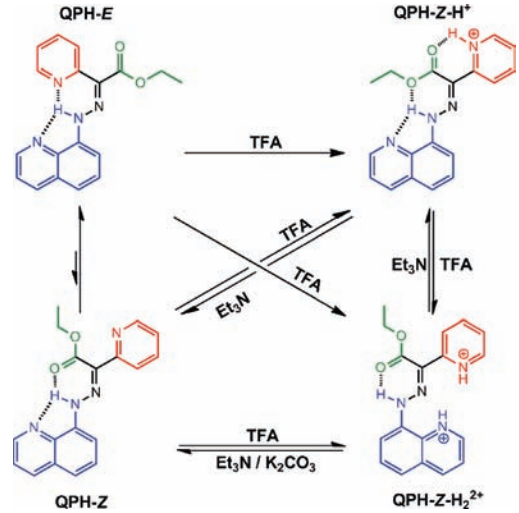

The addition of 2.4 equiv of TFA to **QPH-*E*** in CD_3CN leads to the complete protonation of the pyridyl group (Figure 1b), which is accompanied by a color change from bright yellow to brown. The protonation is expected to break the H-bond and promote rotation[16] about the C═N double bond to give **QPH-*Z*-**H^+, in which the ester group is H-bonded to the hydrazone N−H proton. The ^{1}H NMR spectrum shows that the hydrazone N−H proton signal is shifted to 14.15 ppm[17] indicating the formation of the N−H···O H-bond.[18] Moreover, the pyridyl protons (H9, H10 and H11) are shifted downfield as a result of

(4) (a) Wang, W.; Kaifer, A. E. *Angew. Chem., Int. Ed.* **2006**, *45*, 7042–7046. (b) Nijhuis, C. A.; Ravoo, B. J.; Huskens, J.; Reinhoudt, D. N. *Coord. Chem. Rev.* **2007**, *251*, 1761–1780. (c) Juluri, B. K.; Kumar, A. S.; Liu, Y.; Ye, T.; Yang, Y.-W.; Flood, A. H.; Fang, L.; Stoddart, J. F.; Weiss, P. S.; Huang, T. J. *ACS Nano* **2009**, *3*, 291–300. (d) Parimal, K.; Witlicki, E. H.; Flood, A. H. *Angew. Chem., Int. Ed.* **2010**, *49*, 4628–4632.

(5) (a) Balzani, V.; Credi, A.; Venturi, M. *Pure Appl. Chem.* **2003**, *75*, 541–547. (b) Kottas, G. S.; Clarke, L. I.; Horinek, D.; Michl, J. *Chem. Rev.* **2005**, *105*, 1281–1376. (c) Eelkema, R.; Pollard, M. M.; Vicario, J.; Katsonis, N.; Ramon, B. S.; Bastiaansen, C. W. M.; Broer, D. J.; Feringa, B. L. *Nature* **2006**, *440*, 163. (d) Muraoka, T.; Kinbara, K.; Aida, T. *Nature* **2006**, *440*, 512–515. (e) Russew, M.-M.; Hecht, S. *Adv. Mater.* **2010**, *22*, 3348–3360.

(6) Schilwa, M., Ed. *Molecular Motors*; Wiley-VCH: Weinheim, Germany, 2003.

(7) (a) Kelly, T. R.; de Silva, H.; Silva, R. A. *Nature* **1999**, *401*, 150–152. (b) Leigh, D. A.; Wong, J. K. Y.; Dehez, F.; Zerbetto, F. *Nature* **2003**, *424*, 174–179. (c) Hernández, J. V.; Kay, E. R.; Leigh, D. A. *Science* **2004**, *306*, 1532–1537. (d) Fletcher, S. P.; Dumur, F.; Pollard, M. M.; Feringa, B. L. *Science* **2005**, *310*, 80–82. (e) Dahl, B. J.; Branchaud, B. P. *Org. Lett.* **2006**, *8*, 5841–5844. (f) Feringa, B. L. *J. Org. Chem.* **2007**, *72*, 6635–6652. (g) Kelly, T. R.; Cai, X.; Damkaci, F.; Panicker, S. B.; Tu, B.; Bushell, S. M.; Cornella, I.; Piggott, M. J.; Salives, R.; Cavero, M.; Zhao, Y.; Jasmin, S. *J. Am. Chem. Soc.* **2007**, *129*, 376–386.

(8) We are distinguishing here between *configurational* and *conformational* rotation for the simple fact that energy barriers required for these two processes are quite different. For example, in this manuscript we report that the configurational change (*Z*/*E* isomerization) has a barrier of $\Delta G^{\ddagger}_{294.15K}$ = 24.0 kcal mol^{-1}, whereas the rotation around the C−N single bond (conformational change) is too fast to be monitored using NMR spectroscopy ($\Delta G^{\ddagger}_{294.15K}$ < 5 kcal mol^{-1}). These differences in isomerization rates can be very important in future applications.

(9) Qu, D.-H.; Feringa, B. L. *Angew. Chem., Int. Ed.* **2010**, *49*, 1107–1110.

(10) Whitesides, G. M.; Ismagilov, R. F. *Science* **1999**, *284*, 89–92.

(11) Stoddart, J. F. *Nat. Chem.* **2009**, *1*, 14–15.

(12) Landge, S. M.; Aprahamian, I. *J. Am. Chem. Soc.* **2009**, *131*, 18269–18271.

(13) In the crystal structure of **QPH-*E***, the dihedral angle between the pyridyl ring and the quinolinyl ring is 10.453(48)°, and the torsion angles of N−N═C−C (pyridyl) and C═N−N−C (quinolinyl) are 2.516(279)° and −175.253(161)°, respectively.

(14) (a) Vickery, B.; Willey, G. R.; Drew, M. G. B. *J. Chem. Soc., Perkin Trans. 2* **1981**, 1454–1458. (b) Drew, M. G. B.; Vickery, B.; Willey, G. R. *Acta Crystallogr., Sect. B: Struct. Sci.* **1982**, *38*, 1530–1535. (c) Frohberg, P.; Drutkowski, G.; Wagner, C. *Eur. J. Org. Chem.* **2002**, 1654–1663.

(15) This ratio is less than what was observed (97:3) for our previously reported naphthyl-based system (see ref 12). This observation might arise from the additional H-bond between the N−H proton and the quinolinyl nitrogen, which can stabilize the *Z* configuration.

(16) The naphthyl-based system (ref 12) showed that the *Z*/*E* isomerization rate is dependent on solvent polarity. This is an indication that the isomerization goes through the rotation mechanism and not the lateral shift one: (a) Tobin, J. C.; Hegarty, A. F.; Scott, F. L. *J. Chem. Soc. B* **1971**, 2198–2202. (b) Wong, J. L.; Zady, M. F. *J. Org. Chem.* **1975**, *40*, 2512–2516. (c) Pichon, R.; Le Saint, J.; Courtot, P. *Tetrahedron* **1981**, *37*, 1517–1524.

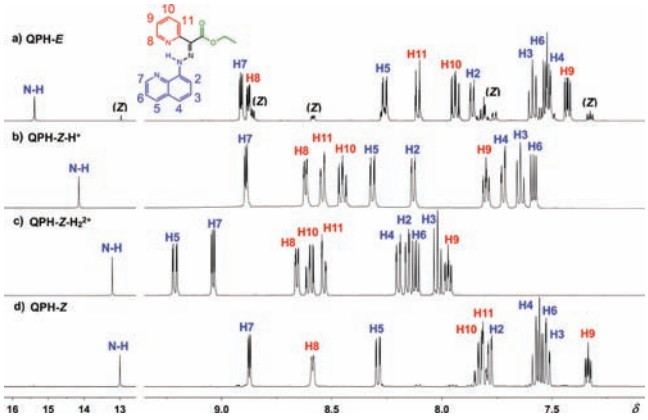

Figure 1. ^{1}H NMR spectra (500 MHz, 294 K) in CD_3CN of (a) **QPH-*E*** with peak assignments (the signals of the minor *Z* isomer are labeled as well); (b) **QPH-*Z*-H$^+$** with peak assignments, recorded after the addition of 2.4 equiv of TFA to **QPH-*E***; (c) **QPH-*Z*-H$_2^{2+}$** with peak assignments, recorded after the addtion of 64 equiv of TFA to **QPH-*E***; (d) **QPH-*Z*** with peak assignments, recorded after passing **QPH-*Z*-H$^+$** through a plug of K_2CO_3.

its protonation,[19] and the signal for proton H8 is shifted upfield from 8.84 to 8.62 ppm, indicating that the pyridyl group is no longer under the influence of the quinolinyl group's ring current effect.[20] The protons on the quinolinyl group are barely affected except for H2, which shifts from 7.82 to 8.14 ppm, in accordance with the protonation of the pyridyl group. The 1D NOESY spectra of **QPH-*Z*-H$^+$** (see SI Figures S9 and S11, Supporting Information) show NOE correlations between (i) protons H2 and H11 and (ii) proton H7 and the methyl group protons, clearly indicating the configuration and conformation of **QPH-*Z*-H$^+$**. The latter interaction is possible only if the ester oxygen is directed toward and H-bonded with the hydrazone N−H proton. This type of an interaction in such hydrazone systems is unprecedented, and it shows the effect of slight structural changes on the system's behavior. The crystal structure of **QPH-*Z*-H$^+$** (see SI Figure X-ray S2, Supporting Information) provides more supporting evidence for this conclusion showing the H-bond between the hydrazone N−H proton and the oxygen atom of the ester group (N−H···O, 2.5732(24) Å, 128.352(1900)°).[21] Moreover, the H-bond between the hydrazone N−H proton and the quinolinyl nitrogen atom (N−H···N, 2.6390(24) Å, 107.529(1778)°) is slightly strengthened while the whole molecule still remains planar.[22]

When the amount of TFA is increased to 10 equiv no significant change is observed in the ^{1}H NMR spectrum. However, beyond 10 equiv, the color of the solution changes from brown to light yellow and a downfield shift is observed for all the aromatic proton signals (Figure 1c), which reaches saturation at 64 equiv. The shift is more pronounced for protons H2−7 of the quinolinyl group: proton signals H3, H4, H5 and H6 are shifted to 8.03, 8.20, 9.22, and 8.13 ppm, respectively, while proton H2 signal is slightly shifted to 8.16 ppm. These shifts clearly indicate the protonation of the quinolinyl group.[23] Meanwhile, the signal of the hydrazone N−H proton is shifted upfield to 13.22 ppm, indicating that it is H-bonded with the ester group.[24] The protonation of the quinolinyl group is anticipated to drive it around the C−N single bond in order to avoid the hydrazone N−H proton. In this new conformation, the quinolinyl nitrogen proton could possibly H-bond with the C═N nitrogen atom, which would generate a stable six-membered ring. A clear NOE correlation is observed in the 1D NOESY NMR spectrum of **QPH-*Z*** (see SI Figure S14, Supporting Information) between proton H2 and the hydrazone N−H proton, which has not been observed for either **QPH-*E*** or **QPH-*Z*-H$^+$**, confirming that the quinolinyl group has flipped over during the second protonation.[25]

In addition, an NOE correlation between proton H11 and the methyl group protons suggests that the protonated pyridyl group adopts an orientation in which the pyridyl nitrogen proton is directed toward the quinolinyl group, and that the hydrazone N−H proton is H-bonded with the carbonyl group. Given the slight difference in the pK_a between the pyridyl group and the quinolinyl group (pK_a 5.17 and 4.85, respectively),[26] it is rather astonishing to observe two distinct protonation/switching steps rather than an equilibrium. Having a doubly positive charged molecule and a H-bonded quinolinyl nitrogen atom makes the second protonation very difficult, which is actually helpful in the precise control of the molecular motion.

Both protonation-driven switching processes can be fully reversed, either by the addition of triethylamine (Et_3N) to the **QPH-*Z*-H$^+$** or **QPH-*Z*-H$_2^{2+}$** solutions, or by passing them through a plug of potassium carbonate (K_2CO_3). After depro-

(17) The chemical shift of the N−H proton is influenced by the ring current effects of the naphthyl moiety, in addition to resonance assisted hydrogen-bonding (RAHB). For RAHB, please see: (a) Bertolasi, V.; Gilli, P.; Ferretti, V.; Gilli, G. *J. Am. Chem. Soc.* **1991**, *113*, 4917–4925. (b) Bertolasi, V.; Gilli, P.; Ferretti, V.; Gilli, G.; Vaughan, K. *New J. Chem.* **1999**, *23*, 1261–1267. (c) Simůnek, P.; Svobodová, M.; Bertolasi, V.; Pretto, L.; Lyčka, A.; Macháček, V. *New J. Chem.* **2007**, *31*, 429–438. These effects impede the direct comparison between the N−H chemical shifts of the different **QPH** isomers. Moreover, they complicate the analysis of the effect that the extra H-bond with the quinolinyl moiety has on the N−H proton, making the direct comparison with the previously published naphthyl-based system (ref 12), very difficult.

(18) The **QPH-*E*/QPH-*Z*-H$^+$** isomerization process is too fast to be monitored by NMR spectroscopy, see ref 12.

(19) Pretsch, E., Ed. *Tables of Spectral Data for Structure Determination of Organic Compounds*; Springer-Verlag: Berlin, Germany, 1989; Vol. 2.

(20) The chemical shift of the equivalent proton to H8 in the starting material (ethyl-2-pyridylacetate) is 8.49 ppm. This clearly shows that proton H8 in **QPH-*E*** is influenced by both RAHB (see ref 17) and the ring current effect of the quinolinyl moiety. The chemical shift of proton H8 in **QPH-*Z*** (8.60 ppm) lends further support to this conclusion.

(21) The observed NOE correlation between protons H2 and H11 shows that in solution, the protonated pyridyl group adopts the orientation in which H11 is directed towards the quinolinyl group, while the crystal structure of **QPH-*Z*-H$^+$** shows that the pyridyl nitrogen proton is directed towards the quinolinyl group. This difference in orientation might stem from crystal packing considerations.

(22) In the crystal structure of **QPH-*Z*-H$^+$**, the dihedral angle between the pyridyl ring and the quinolinyl ring is 2.273(59)°, and the torsion angles of N−N═C−C (pyridyl) and C═N−N−C (quinolinyl) are 179.380(185)° and − 178.483(200)°, respectively.

(23) Barbieri, G.; Benassi, R.; Lazzeretti, P.; Schenetti, L.; Taddei, F. *Org. Magn. Resonance* **1975**, *7*, 451–454.

(24) Mitchell, A. D.; Nonhebel, D. C. *Tetrahedron Lett.* **1975**, 3859–3862.

(25) These systems usually adopt a planar structure that increases their π-delocalization, which in turn leads to resonance-assisted hydrogen bonding (ref 17). This behavior, the possibility of forming a six-membered H-bonded ring, in addition to the acquired NMR and UV-vis data, make us conclude that **QPH-*Z*-H$_2^{2+}$** has a locked planar conformation as depicted in the figures.

(26) Hosmane, R. S.; Liebman, J. F. *Struct. Chem.* **2009**, *20*, 693–697.

tonation, both species return to the initial equilibrium state (see SI Figure S25, Supporting Information) through the metastable form of **QPH-*Z*** (Figure 1d), which is the minor component under equilibrium. The isomerization rate from **QPH-*Z*** to **QPH-*E*** was determined to be $(4.80 \pm 0.05) \times 10^{-6} s^{-1}$ ($\Delta G^{\ddagger}_{294.15K} = 24.0 \pm 0.1$ kcal mol^{-1}), which is much slower than our previously reported[12] naphthyl-based system.[27] The rate change can be attributed to the additional H-bond between the hydrazone N−H proton and the quinolinyl nitrogen atom that stabilizes the **QPH-*Z*** isomer. Moreover, by controlling the amount of Et_3N added, **QPH-*Z*-**H_2^{2+} can undergo monodeprotonation and be switched back to **QPH-*Z*-**H^+ (see SI Figure S25b, Supporting Information), giving us full control over the switching cycle. The rotation rate of the quinolinyl group after the first deprotonation of **QPH-*Z*-**H_2^{2+} is too fast to be monitored by NMR spectroscopy.

Scheme 2. Schematic Depiction of the Switching Sequence of **QPH-*E*** Showing the Rotation around the Two Different Axles

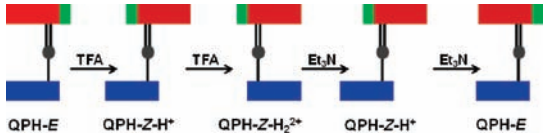

The fact that we can address each one of the four possible states based on the addition sequence of acid and base, gives us full control over the configuration and conformation around two different bonds. In order to demonstrate this, we have conducted the switching sequence depicted in Scheme 2, and used UV−vis spectroscopy to follow the process (Figure 2). The solution of **QPH** in CH_3CN, after reaching equilibrium, has an absorption maximum at $\lambda_{max} = 393$ nm (Figure 2a), and upon titration with TFA (25 equiv) it shifts bathochromically to $\lambda_{max} = 423$ nm to give **QPH-*Z*-**H^+. Titration with 100 equiv of TFA causes no additional change to the spectrum (Figure 2b). However, when the amount of TFA is increased to about 1000 equiv, the absorption profile changes again: the absorption maximum shifts hypsochromically to $\lambda_{max} = 395$ nm and the extinction coefficient decreases drastically, a process that eventually reaches saturation at about 8000 equiv of TFA (Figure 2c) giving **QPH-*Z*-**H_2^{2+}. On the other hand, when the compound is titrated with triflic acid, which is a much stronger acid than TFA,[28] only about 1.2 and 136 equiv are needed to reach the first and second protonation, respectively (see SI Figure S30, Supporting Information).[29] Two different sets of isosbestic points can be clearly observed,[30] indicating that there are only two species in the solution for each step. The two steps of protonation/switching are even more distinctive in the UV−vis spectroscopy study since the concentration is 1,000

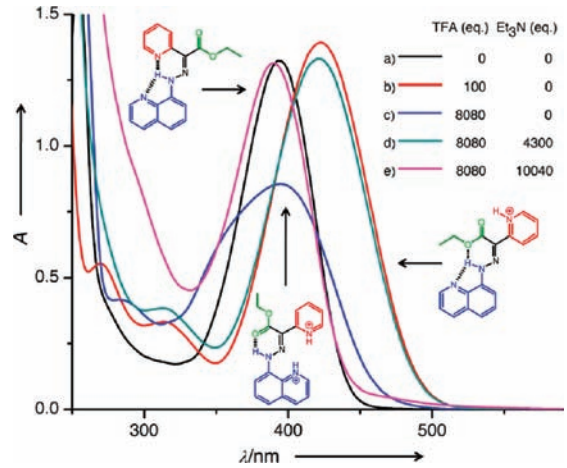

Figure 2. Changes in the UV−vis spectra during the acid/base switching of **QPH**. All data were recored in CH_3CN at 298 K. To a 5.0×10^{-5} M solution of (a) **QPH**, TFA was added to (b) 100 equiv and (c) 8080 equiv until no further change was observed. Et_3N was then added to switch the system back to (d) **QPH-*Z*-**H^+, and then (e) **QPH**.

times lower than that for the NMR measurements. Titration of **QPH-*Z*-**H_2^{2+} with Et_3N reverts it back to **QPH-*Z*-**H^+ (Figure 2d), which then can be converted into **QPH-*E*** via **QPH-*Z*** (Figure 2e and SI Figure S29, Supporting Information), thus completing the full switching cycle.

In summary, an easily accessible chemically activated rotary switch has been synthesized. This system undergoes a four-step switching process in which the *configuration* and *conformation* around different axles can be modulated. We have successfully controlled an intricate motion in a simple molecular switch, and demonstrated that achieving complex motion on the molecular level does not necessitate complicated molecules. This prototype molecular switch can have very promising applications (e.g., in molecular logic[31]) and it expands the molecular tool-box available for us for the construction of advanced molecular devices.

Acknowledgment. This work was supported by Dartmouth College and the Burke Research Initiation Award. We thank Wayne T. Casey for help with NMR spectroscopy and Dr. Richard Staples (Michigan State University) for X-ray analysis.

Supporting Information Available: Experimental procedures, NMR spectra, UV−vis spectra, and crystal structural data for **QPH-*E*** and **QPH-*Z*-**H^+ (CIF). This material is available free of charge via the Internet at http://pubs.acs.org.

OL102422H

(27) The isomerization rate can be enhanced by either heating the sample, or as unpublished preliminary results indicate, by the addition of excess base to the solution that seems to catalyze the *Z*/*E* isomerization.

(28) The pK_a values of TFA and triflic acid in CH_3CN are 12.65 and 2.6, respectively: Eckert, F.; Leito, I.; Kaljurand, I.; Kütt, A.; Klamt, A.; Diedenhofen, M. *J. Comput. Chem.* **2009**, *30*, 799–810.

(29) We are showing the data with TFA to be consistent with the NMR spectroscopy data, which afforded sharper spectra with TFA than triflic acid.

(30) The first protonation process has isosbestic points at $\lambda = 268$, 338, and 405 nm, and the second protonation process has isosbestic points at $\lambda = 284$, 213, and 391 nm.

(31) (a) de Silva, A. P.; Uchiyama, S. *Nat. Nanotechnol.* **2007**, *2*, 399–410. (b) Pischel, U. *Aust. J. Chem.* **2010**, *63*, 148–164.